Duan *et al.*
Chinese Journal of Mechanical Engineering (2024) 37:8
https://doi.org/10.1186/s10033-023-00989-0

Chinese Journal of Mechanical Engineering

ORIGINAL ARTICLE

Open Access

A Novel On-Site-Real-Time Method for Identifying Characteristic Parameters Using Ultrasonic Echo Groups and Neural Network

Shuyong Duan[1*], Jialin Zhang[1], Heng Ouyang[1], Xu Han[1] and Guirong Liu[2]

Abstract

On-site and real-time non-destructive measurement of elastic constants for materials of a component in a in-service structure is a challenge due to structural complexities, such as ambiguous boundary, variable thickness, nonuniform material properties. This work develops for the first time a method that uses ultrasound echo groups and artificial neural network (ANN) for reliable on-site real-time identification of material parameters. The use of echo groups allows the use of lower frequencies, and hence more accommodative to structural complexity. To train the ANNs, a numerical model is established that is capable of computing the waveform of ultrasonic echo groups for any given set of material properties of a given structure. The waveform of an ultrasonic echo groups at an interest location on the surface the structure with material parameters varying in a predefined range are then computed using the numerical model. This results in a set of dataset for training the ANN model. Once the ANN is trained, the material parameters can be identified simultaneously using the actual measured echo waveform as input to the ANN. Intensive tests have been conducted both numerically and experimentally to evaluate the effectiveness and accuracy of the currently proposed method. The results show that the maximum identification error of numerical example is less than 2%, and the maximum identification error of experimental test is less than 7%. Compared with currently prevailing methods and equipment, the proposefy the density and thickness, in addition to the elastic constants. Moreover, the reliability and accuracy of inverse prediction is significantly improved. Thus, it has broad applications and enables real-time field measurements, which has not been fulfilled by any other available methods or equipment.

Keywords Parameter identification, Ultrasonic echo group, High-precision modeling, Artificial neural network, NDT

1 Introduction

The performance and reliability of machinery equipment working in complex and important situations is critical to the operation of the system and need to be evaluated in real time [1, 2]. However, the characteristic parameters based on the actual assessment are often uncertain, resulting in deviations in the assessment, which are mainly manifested in the following aspects: (1) there is deviation between the characteristic parameters referenced by the initial design and the actual parameters after processing and molding [3–5]; (2) some mechanical equipment in service for many years may have local mechanical degradation in key parts, which leads to local changes in the actual characteristic parameters; (3) some large-size structural components can only use artificial processing methods during machining, which will lead to local inconsistency of material and structural characteristic parameters. Therefore, real-time accurate and non-destructive identification of the characteristic parameters

*Correspondence:
Shuyong Duan
duanshuyong@hebut.edu.cn
[1] State Key Laboratory of Reliability and Intelligence of Electrical Equipment, Hebei University of Technology, Tianjin 300401, China
[2] Department of Aerospace Engineering and Engineering Mechanics, University of Cincinnati, Cincinnati 45221, USA

is particularly important for the mechanical performance and reliability assessment of complex equipment [6–8].

With the development of computer technology and numerical simulation methods, more and more researchers choose to apply computational inverse techniques for nondestructive identification of characteristic parameters of components. The computational inverse technique uses the measured responses of a known excitation (load) on a structural system to search the characteristic parameters by solving the physical system as an inverse problem [9, 10]. Usually, impulsive excitation or continuous excitation (high frequency) is applied as the excitation of the system [11]. Amongst, the dynamic methods using pulse excitation to study the vibration characteristics of elastic structures is termed as vibration test method [12]. The specimens are usually subjected to mechanical and elastic impact with an impactor (hammer, etc.) as specified in the ASTM isotropic material test standard [13]. Specifically, Hwang et al. [14] proposed a method combining vibration testing with numerical method to identify the elastic constants of aluminum and carbon / epoxy resin materials. Xu et al. [15] presented an iterative method to derive the mechanical parameters of metal fiber laminate based on the frequency response function with least square method. Duan et al. [16] proposed a method to quantitatively identify the joint stiffness parameters of a robotic arm in real time via measuring the low-order natural frequencies of the robotic arm and the two-way Tubenets theory. To address the uncertainties of the joint stiffness in the robotic arm, Duan et al. [17] identified the uncertain parameters of the joint stiffness in the robotic arm based on the natural frequency of the robotic arm itself. This study of parameter identification based on intrinsic frequencies obtained through impulsive excitation usually is effective in the low frequency range to derive global dynamic behavior. However, the overall mechanical response fails to reflect local mechanical properties and parameter variations. Meanwhile, the dynamic method is also very sensitive to the boundary conditions and response locations of the tested components [18, 19], which are usually ambiguous to be specified. Therefore, the dynamic methods are generally restrained from general application in practical engineering.

Compared to dynamic methods, the ultrasonic wave is mainly in the high frequency band and the stress range is small, which can well reflect the influence of different mechanical properties of the elastic phase on the ultrasonic propagation process. For this reason, the ultrasonic wave is more suitable than the vibration tests for the characterization of field materials [20, 21]. The wave acting on a thin plate or shell structure produces guided propagation between two parallel free surfaces of the material, so it is called a guided wave alias a lamb waves [22, 23]. The guided wave based approach is usually the preferred method for thin plate analysis, which is widely used in the parameter identification of composite plates. Chimenti et al. [24] discussed the generation and detection of guided waves in composite materials and employed dispersion curves to evaluate the material parameters. Pabisek et al. [25] presented a hybrid material identification computational system applying Lamb waves dispersion curves and neural networks to estimate the material parameters. Cui et al. [26, 27] successively extended the numerical work to actual parts tested experimentally and applied a semi-analytic finite element method to identify the elastic coefficients of composite laminates by matching the phase velocity dispersion curves in the direction of single wave propagation. It is understood that the lamb wave mainly propagates in the thin plate in the transverse direction. When the ultrasonic wave is emitted back in the incident wave direction after hitting the bottom boundary. Analysis for the complex dispersion characteristics of the wave is thus spared. On the other hand, once the structure of the specimen is not a thin plate structure, the lamb wave will not be a feasible approach.

For the ultrasonic echo method, the travel time of the ultrasonic echo is often engaged to calculate the velocity of the wave and thus inverse the elastic constant of the material [28–31]. In the 1950s, researchers [32, 33] applied the ultrasonic pulse excitation method to obtain the echo velocity and measure the elastic constants. For example, Hu et al. [34] measured the propagation velocity of ultrasonic waves and calculated the elastic constants using an ultrasonic transducer in order to measure the variation of the elastic constants of aluminum alloy materials at different temperatures. Franco et al. [35] determined the elastic modulus and Poisson's ratio of high-purity aluminum, electrolytic copper and glass by adopting the transverse and longitudinal wave velocities of ultrasonic waves propagating in materials. Besides, Santoni et al. [36] ignored the size and boundary conditions of the laminate by fitting the experimental flexural wave velocity to the dispersion relation to invert the elastic and stiffness properties of the cross-laminated wood. Although many techniques have been developed to identify elastic constants based on the wave velocity of ultrasonic echoes, the applications are very much limited by the prerequisites of the density or thickness of the material, the accurate measurements of longitudinal and transverse wave velocities. To this gap, Liu et al. [37–39] used the hybrid numerical method to calculate the displacement response of elastic waves in the form of the wave group, and combined with a progressive neural network to characterize the material parameters

of anisotropic materials. This method does not require inverse parameterization by wave velocity, but since the displacement response of waves is often intricate to measure, so Liu's study is still held back for numerical simulation stage only [40].

General application of the existing researches are highly limited by ambiguous boundary conditions, non-homogeneity of material properties, prior knowledge of density and thickness, etc. Thus, it is not feasible to identify parameters in real time and on site. To address these issues, this paper proposes a characteristic parameter identification method using ultrasonic echo group signal combined with artificial neural network inverse techniques. This method does not require prior input of density and thickness. Instead, the density and thickness can be treated as target resultants. It enables on-site real-time identification of local characteristic parameters of structural components. To start with, the initial finite element model of the generic ultrasonic echo group is established. The experimental system of ultrasonic echo acquisition is built for validation. A progressive grid search optimization method is then used to update the generic ultrasonic echo group finite element model to refine the finite element model and eliminate the uncertainty interference in the acquisition device. For exemplification, the aluminum alloy material is studied for optimal Latin hypercube sampling in its parameter interval. Material parameter-echo group dataset is generated using numerical simulation technique to train the neural network inverse model. Once the neural network has been trained, the measured echo group waveforms can be used as input parameters to identify the characteristic parameters of the material.

2 Presentation of the Method

The current existing method of identifying elastic constants by ultrasonic wave velocity requires accurate measurement of the propagation time of longitudinal and transverse waves, and mostly uses higher frequency ultrasonic waves for measurement, for example, a frequency of about 5 MHz. The smaller wavelength of the echo is ensured, and the time of arrival of the echo can be determined more easily. In order to accurately count the time interval between multiple echo signals, usually choose the thickness of 20 mm or more specimens for measurement. However, the high frequency signal is accompanied by greater attenuation, which makes it difficult to apply in particularly thick materials and also to penetrate to the lowest layers of the composite. In order to be applicable to more complex situations, consider using longer wavelength ultrasound waves for measurements at lower frequencies. However, a longer wavelength makes the echo signal not a single waveform, instead it is a waveform composed of a more complex group of waves. This complex wave group is difficult to determine the exact time of arrival of the echo, so the existing methods of using wave speed to identify the characteristic parameters are helpless [41]. Only by using advanced numerical simulation techniques combined with neural networks can the analysis of complex wave groups be performed and the characteristic parameters be extracted from the wave groups. So this paper proposes a method to identify the characteristic parameters by ultrasonic echo swarm and neural network. The difficulty of this method is to obtain a repeatable and insensitive wave cluster signal to the shape and structure of the specimen. Therefore, the first few waveform signals in the wave group signal are selected as the input responses of the neural network for prediction.

The flow chart of the currently proposed method is shown in Figure 1. The method is divided into two stages, which are building the generic ultrasonic echo group model and parameter identification via ultrasonic echo group.

In building the generic ultrasonic echo group model, it is a premise to build the basic numerical model and construct an experimental platform for validation. Thus, sensitivity analysis is performed using the numerical model to evaluate the feasibility of adopting the inverse solution technique for identification. Since various uncertainties may exhibit in the modeling process to negate

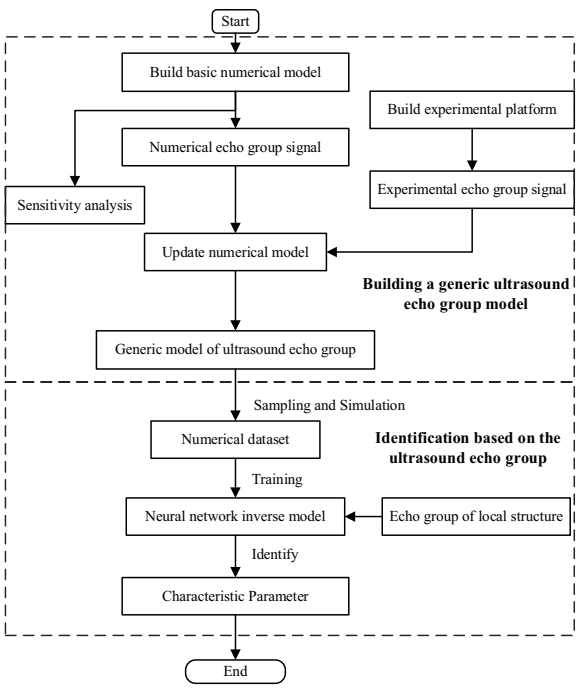

Figure 1 Flow chart for currently proposed method for identification of characteristic parameters

the modeling accuracy, the model should be updated to derive a high-precision generic ultrasonic echo group numerical model. The specific numerical model updating process will be described in detail in Section 3. In the stage of parameter identification via ultrasonic echo group, firstly, the numerical dataset of echo group-characteristic parameters is generated using a high-precision generic ultrasonic echo group numerical model instead of the experimental acquisition of echo signals. The neural network is trained using the numerical dataset. Once the neural network is trained, the experimentally acquired echo group are then input to the inverse model of the trained neural network for parameter identification.

3 Identification of Characteristic Parameters via Echo Group of Ultrasound

3.1 Numerical Modeling of Generic Ultrasound Echo Group

The various shapes of structural components in real engineering a generic ultrasonic echo group numerical model with a wide range of application. The process of establishing the generic ultrasonic echo group numerical model is described in detail as below.

3.1.1 Numerical Modeling of Initial Ultrasonic Echo Group

The ultrasonic double crystal probe is selected in this study as the ultrasonic excitation and reception device for on-site real-time acquisition of the echo signal of the component. Figure 2 illustrates the ultrasonic double crystal probe structure working principal diagram. From Figure 2, it has two piezoelectric wafers. One excites the ultrasonic waves, and the other receives ultrasonic waves and converting the acoustic signals into voltage signals. The acoustic beam passes through the delay block and enters the specimen at a certain incidence angle. Between the two delay blocks, there is a cork sound insulation layer to buffer the interference between the two piezoelectric wafers. Thus, the intensity of the interfacial wave is greatly reduced [20]. It greatly reduces the blind area compared to the single crystal probe and thus is more suitable for thin materials.

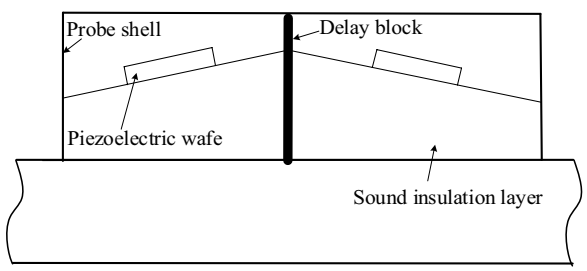

Figure 2 Schematic for double crystal probe

Numerical simulation of the process of acquiring ultrasonic echoes by a double-crystal probe is performed by the finite element software COMSOL to establish a numerical model for the initial ultrasonic echo group. Consequently, a three-dimensional model, as shown in Figure 3a, is built. To reduce the computational intensity of the 3D model, only half of the model is employed in view of symmetry [42, 43]. Part 1 is the test material for simulation of the propagation process of ultrasonic waves. Since the transverse dimension of Part 1 is not the dominating factor for the echo signal, the dimension of the test material is approached by a cylinder with a radius of 25 mm to reduce the computational intensity. 2 mm-thick delamination (Part 4) is deployed on the cylinder side as an absorption layer to mimic an infinite test material.

The double crystal probe is composed of Part 2 and Part 6, which exhibit different functions. The materials and functions for these two parts are shown in Table 1. Specifically, Part 2 is a delay block having an incline angle. Part 3 is the piezoelectric crystal that generates the excitation signal. Part 4 is the sound insulation layer that buffers the interference between the two wafers and Part 5 is the buffer layer that absorbs the residual waves of vibration. Part 6 is the piezoelectric crystal that receives the echo signal. The dimensional parameters of these parts can be seen in Figure 3b.

The overall simulation process of ultrasonic measurement is studied in three steps to investigate the excitation, propagation and reception of ultrasonic signals, respectively. Firstly, the generating excitation ultrasonic waves by a piezoelectric wafer is studied. As shown in Figure 3d, a potential constraint is applied to the upper surface of the excited piezoelectric wafer, which is a 1 MHz DC sinusoidal pulse voltage, and its peak-to-peak value is 200 V. A ground constraint is applied to the lower surface of the excited piezoelectric wafer so that the potential is zero. In the meshing part, the free triangular nodes are employed to mesh the surface of the piezoelectric wafer with a size of 1 mm prior to sweeping along the height direction (Figure 3c). The ultrasonic waves generated by the positive piezoelectric effect are solved using an implicit solver and mapped to the elastic wave study process in the form of pressure loads by a consistent mapping method.

Then the propagation process of ultrasonic waves within the delay block of the probe and the material under test is investigated. The lower surface of the material under test is set as a fixed constraint. A boundary condition of material discontinuity is added between the delay block and the material under test to handle the material property jump. The blue area as shown in Figure 3c is divided into free tetrahedral meshes with the

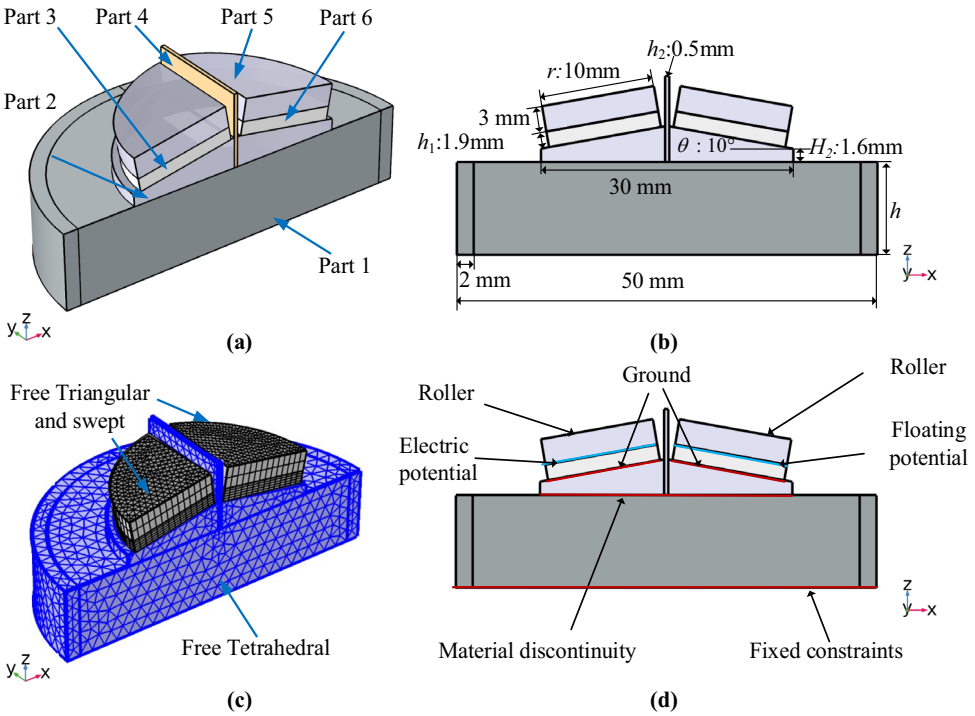

Figure 3 3D model diagram: **a** FE model of generic ultrasound echo groups, **b** Dimensional parameters of FE model, **c** Mesh for finite element model, **d** Setting of boundary conditions

Table 1 Materials and functions of generic ultrasonic echo model components

Parts	Materials	Function
Part 1	Metal	Propagating wave
Part 2	Plexiglass	Delay block
Part 3	PZT-5H	Excited wave
Part 4	Cork	Separating layer
Part 5	Plexiglass	Damping block
Part 6	PZT-5H	Receive wave

maximum mesh size of $\lambda_{min}/1.5$ and a minimum grid size of $\lambda_{min}/2$. Since the main study is the transverse and longitudinal waves propagation in solids and λ_{min} is the wavelength of the transverse wave. The elastic wave study is solved using an explicit solver, which employs the interrupted Galliakin algorithm, and the number of degrees of freedom to be solved is approximately 7.1 million. The computation is performed using a personal computer with CPU i7-8700 and 16G RAM, and the time spent is 3 h.

Finally, the ultrasonic receiving process is simulated. The settings of the grid and the solver are similar to those for the process of the ultrasonic excitation. The boundary condition of the lower surface of the receiving piezoelectric wafer is set to the pressure load, which is the elastic wave pressure load transferred to the lower surface of the receiving piezoelectric wafer in the previous simulation. Setting the upper surface of the receiving wafer as a "floating potential" to collect the voltage signal generated by the inverse piezoelectric effect, a one-dimensional drawing group is created in post-processing to display the voltage signal waveform in real time. It is worth to note that the above divided meshes are only simulated for a single physical field and the loads are mapped by the "consistent mapping" method, so there is no need to consider whether the meshes divided between different studies are aligned on the contact surface.

In order to evaluate the sensitivity of the echo signal to the shape of the specimen, four structures of different shapes as shown in Figure 4a–d, made of aluminum alloy material with a center thickness of 10.5 mm are designed for simulation verification. The time domain signal of the echoes of these four different models is shown in Figure 4e. It can be seen that at the initial moment, the voltage is zero because the ultrasonic waves have not yet reached the receiving piezoelectric sheet. As the ultrasonic waves propagate, the piezoelectric wafer gradually receives the echo signal. In the red dashed box is the first echo that reaches the receiver first, which consists

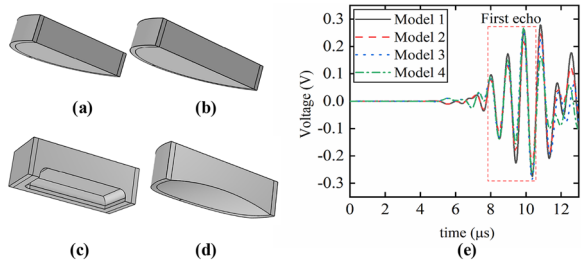

Figure 4 Simulations results: **a** Cylinders with radius of 25 mm, **b** Cylinders with radius of 30 mm, **c** Cuboid with hole in the bottom, **d** Cylinder with radius of 25 mm at the bottom of the surface, **e** Waveform diagram of simulation results

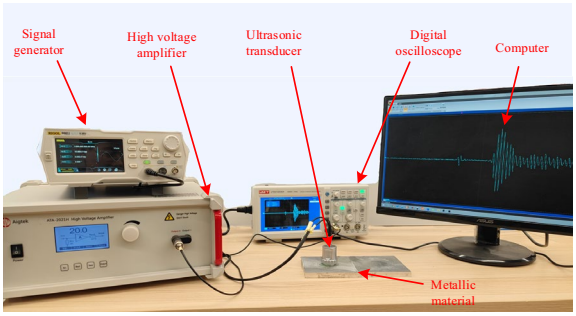

Figure 5 Instruments for experimental system

of a wave group signal with multiple peaks and valleys. The first echoes of the four different models do not differ much from each other. After the first echo, the waveforms start to differ from each other. The reason is that the first echo is the first signal to reach the receiver after the reflection of the ultrasonic waves hitting the bottom boundary, and there is no interference from the clutter reflected from the lateral boundary at this time. This shows that the first echo in the echo group signal is not sensitive to the different transverse boundary of the samples. Since the subsequent arriving waves are full of uncertainties affected by the transverse shape, only the first echo in the echo group signal is viable as the input of the neural network inverse model for identification of the parameters. The first echo signal is only sensitive to the longitudinal propagation path. Thus, as long as the center thickness is the same, the first echo signal remains unchanged. The first echo signal from complex structures, such as curved surfaces, can be approximated using equivalented flat plate. Therefore, the current finite element model based on double crystal probe to acquire the echo signal in this paper is a general ultrasonic echo group numerical model.

3.1.2 Experimental Verification of Ultrasound Echo Group

To verify the reliability of the finite element simulation results, an ultrasonic echo experimental system, as shown in Figure 5 is built. The experimental system is instrumented with the ultrasonic double crystal probe, arbitrary waveform generator, power amplifier, digital oscilloscope, computer, and detected specimen. The ultrasonic double crystal probe is applied to excite the ultrasonic wave and receive the reflected echo signal. It is a Model 1P20FG10 manufactured by Yushi NDT. The center frequency is 1 MHz, the crystal diameter is 20 mm, the focal length is 10 mm. The arbitrary waveform generator RIGOL DG811generates a sinusoidal pulse excitation signal (1 cycle, frequency of 1 MHz). The power amplifier Aigtek ATA-2021H can amplify the voltage to maximum peak-to-peak value of 200 V to meet the voltage requirements for driving the probe. The digital oscilloscope UNI-T UTD2102CEX connects the receiver side of the probe for sampling the ultrasonic waveform. The sampling frequency is 200 MHz, so that the single point sampling time period is 5 ns. The digitized waveform is collected into a personal computer to be processed. In addition, the detected specimen is 100 mm long, 100 mm wide, and 10 mm thick. The operation procedure comprises of mainly four steps as follows.

Step 1. Use sandpaper to smoothen the surface of the specimen, thus mitigating as much as possible the interference of the surface roughness on the ultrasonic signal.
Step 2. Apply an appropriate amount of ultrasonic coupling agent on the center of the specimen surface, so that the ultrasonic waves generated by the probe can be transmitted into the material.
Step 3. Put the probe on the area where the coupling agent is deployed, and press the hand down firmly to record the waveform at this time. Repeat this operation seven times.
Step 4. Process the data for the seven waveform stored in the computer. Remove the waveform with the maximum and minimum values and average the remaining five waveform.

Original waveform of digital oscilloscope collection is shown in Figure 6a. It can be found that the waveform collected directly by the oscilloscope exhibits strong noise interference and should be processed by band pass filtering. Since the center frequency of the experimental excitation signal is 1 MHz, the bandpass interval is set to 0.5–1.5 MHz. It can be seen from Figure 6a that the first waveform attars at 15 μs. This waveform is the interface wave of the double crystal probe itself. The second red dotted circle contains

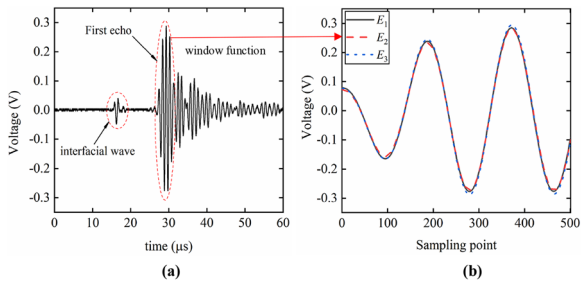

Figure 6 Experimental waveform: **a** Original waveform of digital oscilloscope collection, **b** First echo group waveform after filtering and interception

the large peak of the waveform, which indicates the arrival of the initial echo to the receiving piezoelectric sheet. To isolate the initial echo, a window is added to the measured signal. The waveform is intercepted in the signal interval T_1–T_2 using rectangular window function:

$$x(t) = \begin{cases} 1, T_1 \le t \le T_2, \\ 0, \end{cases} \tag{1}$$

where T_1 is the time point corresponding to the first waveform peak of the first echo in the echo waveform group. The peak of the waveform is traversed from the moment zero, and when the peak is greater than the threshold value of 0.08 V, it is the initial velocity wave, and the time point at this time is T_1. T_2 is the termination point of the intercepted signal, and in order to select the information with three peaks and troughs, T_2 is set here to be at 2.5 μs after T_1, and the amount of information contained in this echo signal satisfies the use of subsequent studies. Since the time interval of each point is 5 ns, 501 data points are sampled in the $T_1 - T_2$ interval. The sampled echo signal graph is shown in Figure 6b. In this interval, the echo signal waveform contains three peaks and valleys, which meets the requirements as the input response. If too few points are sampled, the number of feature points in the waveform will not meet the recognition requirements. If the points are sampled too many, there may be interference from subsequent clutter to negate recognition. Therefore, after comprehend, 501 data points are sampled as the input response of the neural network inverse model. In addition, in Figure 6b, E_1, E_2, and E_3 represent the waveforms measured in three experiments (several days apart), respectively. It can be seen that the errors among these three experiments are minimal, indicating that the acquisition method of this study can effectively reduce the influence of artifacts on the ultrasonic probe measurement results since the results are repetitive.

3.1.3 Process of Updating Numerical Model of Ultrasonic Echo Group

In practical application, the device structure for measuring ultrasonic echoes is subject to various uncertainties with regard to geometry, material parameters, and cognitions. These uncertainties will lead to deviations between the simulation results using nominal structural parameters and the experimental results. The usual practice to reduce such error is to modify the model parameters until the error between analytical predictions and experimental results meets the specified requirements [44–46]. Therefore, after constructing the initial finite element model and the experimental system, the initial ultrasonic echo group numerical model based on the double crystal probe should be updated to improve the relevance of the numerical model.

Assuming that there are n uncertain structural variables, which can be aggregately denoted as $\boldsymbol{x} = (x_1, x_2, \cdots, x_n)$. Sampling in the intervals of these uncertain variables yields m combinations of structural variables χ. The ith sampled combination can be expressed as $\boldsymbol{x}_i$. The structure optimization objective function of the ultrasonic echo group numerical model can then be set as:

$$\begin{cases} \min\limits_{i} \{F(\chi_i)\}, i = 1, 2, \cdots, m, \\ F(\chi_i) = \sum\limits_{j=1}^{k} f(\varepsilon), j = 1, 2, \cdots, k, \\ f(\varepsilon) = \sum\limits_{s=1}^{\tau} \left(\boldsymbol{V}_{ij}^{\mathrm{FEM}} - \boldsymbol{V}_{j}^{\mathrm{EXP}} \right)^2, s = 1, 2, \cdots, \tau, \end{cases} \tag{2}$$

where $\boldsymbol{V}_{ij}^{\mathrm{FEM}} = \left(V_{ij1}^{\mathrm{FEM}}, \cdots, V_{ijs}^{\mathrm{FEM}}, \cdots, V_{ij\tau}^{\mathrm{FEM}} \right)$ indicates the voltage at each time instant s from the simulation; $\boldsymbol{V}_{j}^{\mathrm{EXP}} = \left(V_{j1}^{\mathrm{EXP}}, \cdots, V_{js}^{\mathrm{EXP}}, \cdots, V_{j\tau}^{\mathrm{EXP}} \right)$ represents the voltage per moment s from the experimental acquisition; k denotes the number of materials involved in the test. Since the objective function involves the optimization of a discrete nonlinear problem, solution to the derivative of the objective function is not straightforward. Moreover, the calculation of individual finite element models is intensive, and the overall calculation time can reach hundreds of hours. To reduce the computational intensity, a progressive grid search optimization method is proposed, as shown in Figure 7. The steps for the optimization method can be summarized as follows [47].

Step 1. *Initialization*: Through the sensitivity analysis of the uncertain structural variables, the three most sensitive uncertain variables are identified, which are the thickness h_1 of the piezoelectric film, the thickness h_2 of the retardation block and the inclination angle θ of the retardation block. Initialize the finite element

model and turn these three structural parameters into variables.

Step 2. *Rough sampling*: Based on the initial nominal parameters of the three uncertain variables, the upper and lower bounds of the optimal design of the interval uncertainty are divided. The larger interval of the three uncertain variables is uniformly sampled in large steps.

Step 3. *Finding local optimal point*: The echo signal of the numerical simulation is obtained by parallel calculation of all sample points obtained after coarse selection sampling. The numerical results are input to the structural optimization function (Eq. 2) together with the experimental results, and the objective function values corresponding to the interval sampling points are calculated. The actual situation of two different aluminum alloy materials as shown in Table 2 is taken into account in this step.

Step 4. *Update the local optimum point*: Set a smaller range of intervals around the local optimum and reduce the step size of the search sampling to obtain all sample points. Then find the corresponding local optimum point for updating at this time.

Step 5. *Stopping criteria*: If the fitting accuracy of the current local optimum reaches the set accuracy, i.e., when the value of the objective function is less than 0.5, then the iterative updating process ends and the final optimal structural parameters are obtained, which leads to the optimal finite element model. Otherwise, return to Step 4 to continue the update.

The initial values of the nominal structural parameters of the three uncertainty variables corresponding to the ultrasonic double crystal probe used in this study are 1.9 mm, 1.6 mm, and 10°, respectively. Because the FE simulation is time-consuming, parallelism on multiple computers is implemented. The stopping criterion is reached after the third iteration, when the uncertainty parameter interval has been narrowed down to a smaller range, and it is difficult to further improve the accuracy by making fine parameter corrections. Therefore, only three iterations of interval optimization were performed in this study, and the values of the objective function in the specific iterative optimization process are shown in Figure 8. The interval variation of the uncertain structural parameters, locally optimal structural parameters, locally optimal function values and the time taken are shown in Table 3.

Combination Figure 8 and Table 3 it can be seen that at the first interval sampling, the second set of samples corresponds to the smallest objective function value of 1.23. The corresponding local optimal structure parameters at this time are 1.8 mm, 1.5 mm, and 10°, respectively. Since the maximum optimization interval is set, the local optimal structural parameters are not expanded outside the boundary when they are at the boundary, but the interval is contracted with a single boundary. In the second iteration of the interval, it can be seen that the smallest value of the objective function

Table 2 Material parameters

Species	*E* (GPa)	*υ*	*ρ* (kg/m^3)	*h* (mm)
Al-6061	69	0.33	2700	10.15
Al-7075	71	0.33	2810	10.5

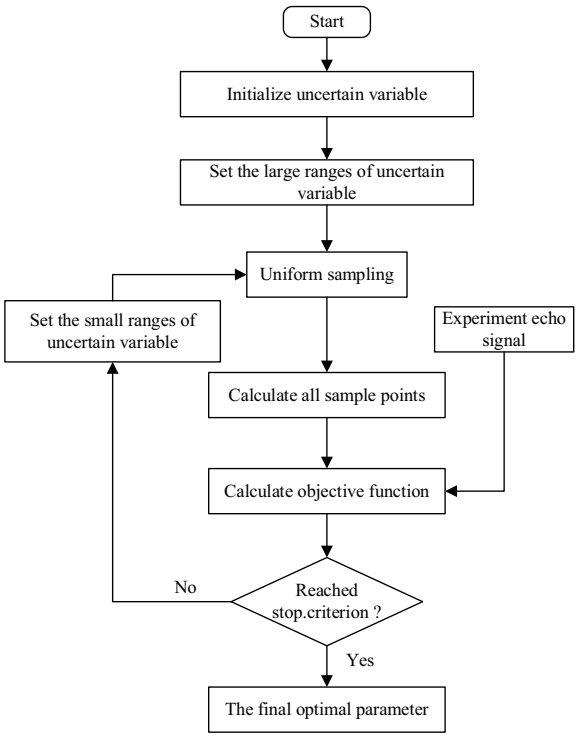

Figure 7 Flowchart for progressive grid search to update FE model

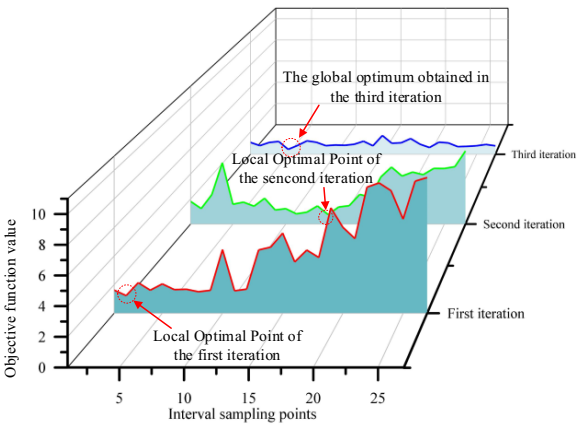

Figure 8 Objective function values for three iterations of interval sampling

Table 3 Results of update FE model

No.	Parameter interval [f^L, f^R] h_1, h_2, θ	Local optimum point	Current optimal function value	Cost time (h)
1	[1.80, 2.0], [1.50, 1.70], [9.60,10.40]	1.80, 1.50, 10.0	1.23	203
2	[1.8, 1.9], [1.5, 1.6], [9.80,10.20]	1.85, 1.55, 10.0	0.77	199
3	[1.80, 2.0], [1.50, 1.70], [9.60,10.40]	1.80, 1.50, 10.0	1.23	203

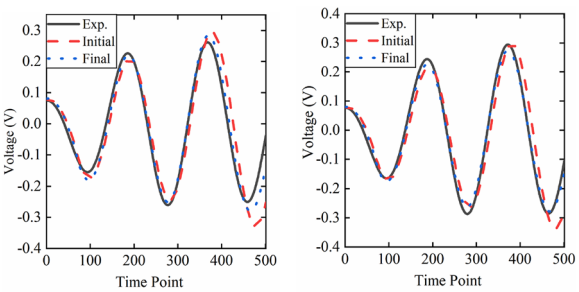

Figure 9 Comparison of iterative results for aluminium alloy materials

corresponding to the 14th sampling group is 0.77. The corresponding local optimal structural parameters at this time are 1.85 mm, 1.55 mm, and 10°, respectively. Then the boundary is contracted again for the third iteration, and the obtained local optimum value is 0.44 less than the set optimization stopping criterion, at which point the structural parameters are the global optimum structural parameters. By using this optimization method, the optimal structural parameters can be obtained in parallel and quickly.

Comparison of the experimental signal waveform with the initial parameter simulation waveform and the optimal parameter simulation waveform after three iterations for two materials is shown in Figure 9. It can be seen that different materials, even the same category of alloys, have different mechanical properties, result in differences in the echo signals. Thus, the waveform signal can be used to invert the material parameters. Comparing the iterated echo signal with the respective initial echo signal, the iterated echo signal fits better with the experimental waveform.

In this study, the effort is concentrated on the introduction of the currently proposed method, thus only the aluminum alloy materials, which do not exhibit strong anisotropic behavior and can well reflect the properties of the actual material, is chosen as the exemplification.

3.2 Identification of Characteristic Parameters via Echo Group of Ultrasound and ANN

After establishing a high-precision generic ultrasonic echo group numerical model based on the double crystal probe, the ultrasonic echo signal corresponding to a specific feature parameter can be obtained by numerical simulations. This numerical model is used to generate a numerical data set, and the neural network is trained to obtain the inverse model of the characteristic parameters. Artificial neural networks compare with the traditional formulation inverse problem approach, the model of feature parameter identification based on neural network can fit various nonlinear relationships without relying on the assumed form of the constitutive equation [48–50]. This inverse process can be represented by the following equation:

$$Y(E, \upsilon, \rho, h) = G(V_R(t)), \tag{3}$$

where $Y(E, \upsilon, \rho, h)$ is the combination of parameters of the material under test $G(\cdot)$; is a nonlinear mapping between the echo time domain signal $V_R(t)$ and a set of corresponding parameter combinations $Y(E, \upsilon, \rho, h)$ fitted by the neural network. The mapping relation is obtained by training the neural network, and the network training process corresponds to the learning process of the function $G(\cdot)$. The training phase continuously reverses the weights and biases of the connections between neurons by known inputs and outputs employing a training algorithm. The error between the predicted value and the actual value is minimized. Several methods are available to train the network, the most prevailing training algorithm is back propagation. This process is also the learning process of the optimal values of the weights and deviations, aiming at an efficient approximation to the piezo/wave propagation behavior. After the training phase, the neural network should be tested with data independent from the training set to verify the generalization ability of the network.

In the network, there are usually several hidden layers with neurons in each layer. As seen in Figure 10b, each neuron has an activation function that increases

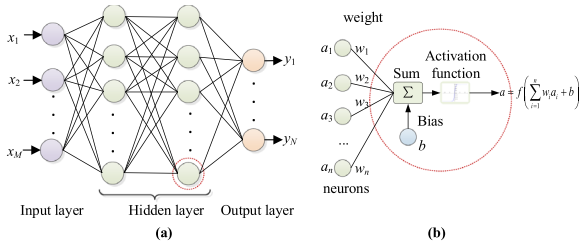

Figure 10 Schematic of ANN: **a** Structural diagram of ANN for parameter identification, **b** Schematic diagram of single neuron

the nonlinear capability of the neural network. The output of the neuron of the previous layer is multiplied by the weights w_i and then summed by a bias b. Using the Python language and based on the TensorFlow framework, the neural network model as shown in Figure 10a is built. The input layer x_M denotes the normalized voltage at each moment corresponding to the echo signal. The output layer y_N is the material parameters after dimensionless processing.

In addition, before the training process, the hyperparameters of the network should be modulated with regard to performance metrics, network structure (number of implied layers, number of nodes in each implied layer), activation function type, learning algorithm, etc [51]. Through thorough debugging, it can be found that, for the mapping relationship between the echo signal and the model parameters in this study, the hyperbolic tangent Tanh function yields better results compared with other activation functions. The Adam optimizer algorithm is also employed as the optimal learning algorithm, which has the advantages of high computational efficiency and smooth descent gradient. The learning rate is set as a dynamic learning rate, which implies that the learning rate will gradually become smaller with the decreasing loss value. This ensures that the overall neural network can be trained efficiently. The loss function is set as

$$Loss = \sum_{i}^{N} \left(\frac{y_i - y_i^{\text{pre}}}{y_i} \right)^2, \tag{4}$$

where y_i is the ith actual feature parameter value corresponding to the structure, and y_i^{pre} is the ith feature parameter value obtained from the neural network prediction. The variations in the data sets lead to differences in the network structure, thus it should be adjusted according to the actual situation. The network structure will be exposited in the following section.

4 Numerical and Experimental Examples

In order to verify the viability and effectiveness of the currently proposed identification method, two numerical cases are designed, and aluminum alloy specimens are selected for experimental verification.

4.1 Numerical Case 1: Known Thickness

It is assumed that the thickness of the structure is known or measurable. Only three parameters of the specimen, i.e., Young's modulus E, Poisson's ratio v, and density ρ, should be identified. To verify the effectiveness of the neural network for parameter identification at different thicknesses, 300 data sets of 10.15 mm and 10.5 mm thickness are generated, respectively.

The aluminum alloy material parameters in Table 2 are used as the reference for interval division, and the bounds of the intervals are ±10%. The interval of Young's modulus is [63, 77] GPa; the interval of Poisson's ratio is [0.3, 0.36]; the interval of density is [2500, 2900] kg/m^3. The sample combinations are then extracted by adopting the optimized Latin hypercube algorithm for sampling (OLHS) in the intervals of these three material parameters. Employing the improved finite element model to calculate these sample combinations, the corresponding echo signal solutions can be obtained. The final data sets with input and output relations are acquired. Since there are scale difference between different material parameters, the parameters are normalized to be dimensionless. It is implemented by dividing by the maximum value of the corresponding parameter. This normalizes the intervals of the three different parameter values to 1 and eliminates the influence of different magnitudes of the parameters.

Randomly selecting 20% of the data samples from the total data samples as the test set, and the remaining 80% as the training set, the batch sizes of both training and test sets are specified to be 16, and the group with the thickness of 10.15 mm converges to a loss of 1.3×10^{-6} after training 80000 epoch times. The group with the thickness of 10.5 mm converges to a loss of 2.3×10^{-7} after training 400000 epoch times. The results of verifying the training effect with the test set are shown in Tables 4 and 5.

From the above two tables, the test results of these two data sets for different heights are satisfactory in view of the maximum recognition effect is below 1%. It demonstrates that this network is feasible and effective to identify three unknown material parameters.

4.2 Numerical Case 2: Unknown Thickness

Assuming that numerical case 2 is an assembled unknown structure, the thickness and material

Table 4 Relative errors of three-parameter numerical test set for 10.15 mm thickness

Relative error	Parameter class		
	E	*υ*	*ρ*
Max (%)	0.55	0.097	0.96
Min (%)	− 0.23	− 0.11	− 0.26
RMS (%)	0.114	0.0387	0.148

Note: ANN structure: 501-100-100-3; activation function Tanh; 240 training samples, 60 test samples; loss=1.3×10^{-6}

Table 5 Relative errors of three-parameter numerical test set for 10.5 mm thickness

Relative error	Parameter class		
	E	*υ*	*ρ*
Max (%)	0.30	0.19	0.21
Min (%)	−0.17	−0.14	−0.11
RMS (%)	0.058	0.033	0.044

Note: ANN structure: 501-100-100-3; activation function Tanh; 240 training samples, 60 test samples; loss=2.3×10^{-7})

Table 6 Relative error of four-parameter numerical test set

Relative error	Parameter class			
	E	*υ*	*ρ*	*h*
Max (%)	1.17	0.54	1.40	0.44
Min (%)	−1.12	−0.39	−1.11	−0.67
RMS (%)	0.362	0.158	0.458	0.176

Note: ANN structure: 501-100-100-4; activation function Tanh; 240 training samples, 60 test samples; loss = 9×10^{-6}

parameters are not to be measured directly. Four model parameters of the metal structure, i.e., Young's modulus E, Poisson's ratio υ, density ρ, and thickness h are to be identified. Similarly, a data set is generated for verification. The thickness interval is set into [9, 11] mm with a nominal thickness of 10 mm. Similar procedure as for the numerical case is again implement to sample data set, and normalize the parameters. Randomly selected 20% of the data set is applied as the test set, and the remaining 80% is employed as the training set. The batch size is set to 16, and the test set loss converges to 9×10^{-6} after 300000 epoch times. The relative errors of the test set are shown in Table 6. It can be seen that the prediction of density is poor in the middle of the four parameters, and the maximum relative error is 1.4%.

By analyzing these two numerical cases, the recognition accuracy for the known height is higher than that of the unknown height. The main reason is that the number of unknown parameters determines the spatial dimension of the parameter distribution, and for each additional unknown parameter, the spatial size of the parameter to be sampled will increase exponentially. This will be more intricate for the neural network to learn. One of the most prevailing method to improve the learning ability of neural networks is to increase the amount of sample data. However, more data sets may not necessarily yield better result. The optimal number of data sets should be explored according to the specific training situation.

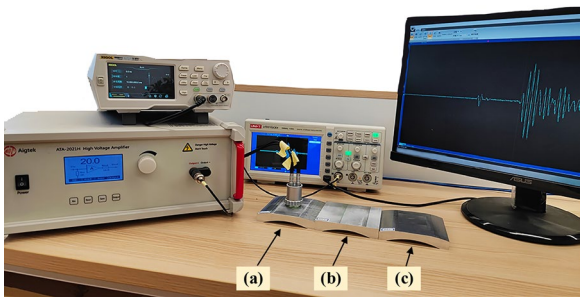

Figure 11 Experiment with curved specimens

4.3 Experimental Example

To further verify the effectiveness of the currently proposed method with structural insensitivity, experiment is performed for the above mentioned two numerical cases. Firstly, the identification effect of the experiments for numerical case 1 with known height is verified. Since the two data sets of numerical case 1 corresponding to the thicknesses of 10.15 mm and 10.5 mm, Al-6061 aluminum alloy plate with the thickness of 10.15 mm and Al-7075 aluminum alloy plate with the thickness of 10.5 mm in Section 3 are selected. The echo waveform of these two aluminum alloy plates collected in Section 3 are input into the corresponding trained neural network for recognition. The recognition accuracy is shown in Figure 12a. It can be seen that the experimental results exhibit larger error (maximum error is around 4%) compared that by the numerical test. To verify the experimental recognition effect of the unknown thickness of numerical case 2, three specimens are selected for experimental tests. The shape and material parameters of these three specimens are shown in Figure 11 and Table 7. Two different aluminum alloy materials are selected for comparative analysis. the Top and bottom surfaces of both specimens (a) and (c) are machined. In order to check the effect of different shapes on the identification accuracy, only the lower surface of specimen (b) is machined.

The implementation steps for experiment approximate those as described in Section 3. Firstly, the surface of the specimen is smoothened with sandpaper. The coupling agent is then attached to the center of the specimen. The probe is pressed downward onto the specimen to record

Table 7 Curved specimen material parameters

	Materials	*E* (GPa)	*υ*	*ρ* (kg/m^3)	*l* × *w* (mm×mm)	*h* (mm)
a	Al-6061	69	0.33	2700	100 × 100	10.65
b	Al-7075	71	0.33	2810	100 × 100	10.37
c	Al-7075	71	0.33	2810	100 × 100	10.70

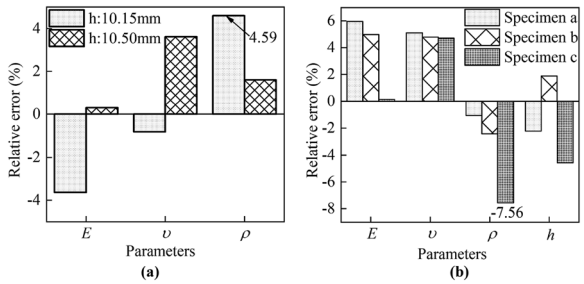

Figure 12 Identification accuracy chart of experimental specimens: **a** Flat specimens, **b** Curved specimens

the waveform. Repeat pressing the probe seven times. The acquired signals are processed to filter out the noise signals. It is worth noting that because of the curved bottom, the center position should be specified precisely to extract the center thickness precisely.

Inputting the processed waveforms into the neural network trained in numerical case 2 for recognition, the recognition accuracy is then shown in Figure 12b. From the figure, it can be stated that the maximum error in the density reaches about 7%. Analyzing the numerical and experimental examples comprehensively, the prediction effect of density in the recognition process is the worst. This may be attributed to the low sensitivity of the density to the echo signal. Compared with the prediction results of the three parameters, the recognition accuracy for the four parameters is not as good either numerically or experimentally. However, four parameters indicate the identification for more complex situations that the currently proposed method can process. It is expected that expansion of the data set can further improve the identification accuracy.

5 Conclusions

In this paper, a parameter identification method via ultrasonic echo group and ANN is proposed. The method combines the advantages of both advanced numerical simulation techniques and ANNs. High-fidelity numerical models instead of an experiments are established to produce datasets for training the neural network. The time domain voltage signal points of the first echo group are used as the input and the characteristic parameters of the structure are output through the ANN. The trained ANN is used to identify the characteristic parameters of the structure. The major conclusions of this study are as follows.

(1) Ultrasonic echoes are more straightforward to acquire than other mechanical responses and are insensitive to transverse boundaries. The ultrasonic double-crystal probe is selected to acquire the ultrasonic echo groups of the structure. A numerical model based on the double-crystal probe is established to compute the echo group signal of a structure.
(2) Uncertainties in the modeling process are minimized. Considering the uncertainty of the double-crystal probe, it can lead to the deviation of the numerical simulation results from the experimental results. To reduce this deviation, the finite element model is updated using a progressive mesh search optimization method to improve the accuracy of the numerical model of the echo group from a generic ultrasound based on a double crystal probe.
(3) The effectiveness and practicality of the proposed method are verified by numerical and experimental examples of aluminum alloy materials. The results show that the maximum error of numerical example is less than 2%, and the maximum error of experimental test is less than 7%. The similar procedure can be extended for other types of materials
(4) Compared with currently prevailing methods and equipment, the proposed method identifies the density and thickness in addition to the elastic constants. Moreover, the reliability and accuracy of inverse prediction are significantly improved.
(5) The proposed method can be used in for portable instruments for parameter identifiers for structures in service.
(6) The currently proposed method can have broad applications and enables real-time measurements.

Acknowledgements
Not applicable.

Authors' Contributions
SD was in charge of the whole trial and reviewed the manuscript; JZ and HO wrote the manuscript; JZ assisted with sampling and laboratory analyses. XH and GL provided ideas and theoretical guidance for the research. All authors read and approved the final manuscript.

Authors' Information
Shuyong Duan, born in 1984, is currently an associate professor at *State Key Laboratory of Reliability and Intelligence of Electrical Equipment, Hebei University of Technology, China*. She received her PhD degree from *Hunan University, China*, in 2016. Her research interests include robot reliability, computational inverse techniques, intelligent robotics.
Jialin Zhang, born in 1998, is currently a master candidate at *State Key Laboratory of Reliability and Intelligence of Electrical Equipment, Hebei University of Technology, China*.
Heng Ouyang, born in 1991, is currently a postdoc at *State Key Laboratory of Reliability and Intelligence of Electrical Equipment, Hebei University of Technology, China*.
Xu Han, born in 1968, is currently a professor and a PhD candidate supervisor at *State Key Laboratory of Reliability and Intelligence of Electrical Equipment, Hebei University of Technology, China*. His main research interests include computational inverse techniques, optimization theory and algorithm.
Guirong Liu, born in 1958, is currently a professor and a PhD candidate supervisor at *Department of Aerospace Engineering and Engineering Mechanics, University of Cincinnati, USA*. His main research interests include computational inverse techniques, intelligent perception of robots, intelligent algorithm, optimization theory and algorithm.

Funding
Supported by National Natural Science Foundation of China (Grant No. 51805141), Funds for Creative Research Groups of Hebei Province of China (Grant No. E2020202142), Tianjin Municipal Science and Technology Plan Project of China (Grant No. 19ZXZNGX00100), Key R & D Program of Hebei Province of China (Grant No.19227208D), National Key Research and development Program of China (Grant No. 2020YFB2009400).

Data availability
The data that support the findings of this study are available on request from the corresponding author, Duan, upon reasonable request.

Declarations

Competing Interests
The authors declare no competing financial interests.

Received: 31 August 2021 Revised: 10 July 2022 Accepted: 21 December 2023
Published online: 19 January 2024

References

[1] S Afshan, O Zhao, L Gardner. Standardised material properties for numerical parametric studies of stainless steel structures and buckling curves for tubular columns. *Journal of Constructional Steel Research*, 2019, 152: 2-11.
[2] X Zhang, Y Chen, J Hu. Recent advances in the development of aerospace materials. *Progress in Aerospace Sciences*, 2018, 97: 22-34.
[3] A H Streppel, L J de Vin, J Brinkman, et al. Suitability of sheet bending modelling techniques in CAPP applications. *Journal of Materials Processing Technology*, 1993, 36(3): 339-356.
[4] F Morestin, M Boivin, C Silva. Elasto plastic formulation using a kinematic hardening model for springback analysis in sheet metal forming. *Journal of Materials Processing Technology*, 1996, 56(1): 619-630.
[5] C Fast-Irvine, A Abedini, J Noder, et al. An experimental methodology to characterize the plasticity of sheet metals from uniaxial to plane strain tension. *Experimental Mechanics*, 2021, 61(9): 1381-1404.
[6] M Yakout, A Cadamuro, M A Elbestawi, et al. The selection of process parameters in additive manufacturing for aerospace alloys. *The International Journal of Advanced Manufacturing Technology*, 2017, 92(5): 2081-2098.
[7] Y Zhong, Y Shan, F Xiao, et al. Effect of toughness on low cycle fatigue behavior of pipeline steels. *Materials Letters*, 2005, 59(14): 1780-1784.
[8] J Janutėnienė, R Didžiokas, M Gintalas. Analysis of the variation of metals mechanical properties depending on operation time. *Mechanics*, 2009, 75(1): 26-30.
[9] G R Liu, X Han. *Computational inverse techniques in nondestructive evaluation*. Boca Raton: CRC Press, 2003.
[10] M Z Siddiqui, S Z Khan, M A Khan, et al. A projected finite element update method for inverse identification of material constitutive parameters in transversely isotropic laminates. *Experimental Mechanics*, 2017, 57(5): 755-772.
[11] J H Tam, Z C Ong, Z Ismail, et al. Identification of material properties of composite materials using nondestructive vibrational evaluation approaches: A review. *Mechanics of Advanced Materials and Structures*, 2017, 24(12): 971-986.
[12] B J Schwarz, M H Richardson. Experimental modal analysis. *CSI Reliability Week*, 1999, 35(1): 1-12.
[13] ASTM International. ASTME1876-09 Standard test method for dynamic Young's modulus, shear modulus, and Poisson's ratio by impulse excitation of vibration. West Conshohocken: ASTM International, 2009.
[14] S Hwang, C Chang. Determination of elastic constants of materials by vibration testing. *Composite Structures*, 2000, 49(2): 183-190.
[15] Z Xu, H Li, W Wang, et al. Inverse identification of mechanical parameters of fiber metal laminates. *Proceedings of the Institution of Mechanical Engineers, Part C: Journal of Mechanical Engineering Science*, 2019, 234(8): 1516-1527.
[16] S Y Duan, L Wang, F Wang, et al. A technique for inversely identifying joint stiffnesses of robot arms via two-way TubeNets. *Inverse Problems in Science and Engineering*, 2021, 29(13): 3041-3061.
[17] S Y Duan, L T Shi, L Wang, et al. An uncertainty inversion technique using two-way neural network for parameter identification of robot arms. *Inverse Problems in Science and Engineering*, 2021, 29(13): 3279-3304.
[18] J Cugnoni, T Gmür, A Schorderet. Inverse method based on modal analysis for characterizing the constitutive properties of thick composite plates. *Computers & Structures*, 2007, 85(17): 1310-1320.
[19] F Daghia, S de Miranda, F Ubertini, et al. Estimation of elastic constants of thick laminated plates within a bayesian framework. *Composite Structures*, 2007, 80(3): 461-473.
[20] J Krautkrämer, H Krautkrämer. *Ultrasonic testing of materials*. Berlin Heidelberg: Springer, 2013.
[21] S M Walley, J E Field. Elastic Wave propagation in materials. *Reference Module in Materials Science and Materials Engineering*, 2016, 1: 1-7.
[22] W G David, J O Irving, Z Peng. Lamb waves and nearly-longitudinal waves in thick plates. *Proc. SPIE*, 2008, 6932: 435-444.
[23] J D Achenbach. *Wave propagation in elastic solids*. Amsterdam: Elsevier, 2012.
[24] D E Chimenti. Guided waves in plates and their use in materials characterization. *Applied Mechanics Reviews*, 1997, 50(5): 247-284.
[25] E Pabisek, Z Waszczyszyn. Identification of thin elastic isotropic plate parameters applying Guided Wave Measurement and Artificial Neural Networks. *Mechanical Systems and Signal Processing*, 2015, 64-65: 403-412.
[26] R Cui, F Lanza di Scalea. On the identification of the elastic properties of composites by ultrasonic guided waves and optimization algorithm. *Composite Structures*, 2019, 223: 110969.
[27] R Cui, F Lanza di Scalea. Identification of elastic properties of composites by inversion of ultrasonic guided wave data. *Experimental Mechanics*, 2021, 61(5): 803-816.
[28] Z A Moradian, M Behnia. Predicting the uniaxial compressive strength and static Young's modulus of intact sedimentary rocks using the ultrasonic test. *International Journal of Geomechanics*, 2009, 9(1): 14-19.
[29] V L d A Freitas, V H C d Albuquerque, E d M Silva, et al. Nondestructive characterization of microstructures and determination of elastic properties in plain carbon steel using ultrasonic measurements. *Materials Science and Engineering: A*, 2010, 527(16): 4431-4437.
[30] V L de Araújo Freitas, P G Normando, V H C de Albuquerque, et al. Nondestructive characterization and evaluation of embrittlement kinetics and elastic constants of duplex stainless steel saf 2205 for different aging times at 425°C and 475°C. *Journal of Nondestructive Evaluation*, 2011, 30(3): 130-136.

[31] Q Pan, R Pan, C Shao, et al. Research review of principles and methods for ultrasonic measurement of axial stress in bolts. *Chinese Journal of Mechanical Engineering*, 2020, 33: 11.
[32] M F Markham. Measurement of elastic constants by the ultrasonic pulse method. *British Journal of Applied Physics*, 1957, 8(S6): S56-S63.
[33] S Eros, J R Reitz. Elastic constants by the ultrasonic pulse echo method. *Journal of Applied Physics*, 1958, 29(4): 683-686.
[34] E Hu, W Wang. The elastic constants measurement of metal alloy by using ultrasonic nondestructive method at different temperature. *Mathematical Problems in Engineering*, 2016, 2016: 6762076.
[35] E E Franco, J M Meza, F Buiochi. Measurement of elastic properties of materials by the ultrasonic through-transmission technique. *Dyna*, 2011, 78(168): 58-64.
[36] A Santoni, S Schoenwald, B Van Damme, et al. Determination of the elastic and stiffness characteristics of cross-laminated timber plates from flexural wave velocity measurements. *Journal of Sound and Vibration*, 2017, 400: 387-401.
[37] G R Liu, J Tani, T Ohyoshi, et al. Transient Waves in Anisotropic Laminated Plates, Part 1: Theory. *Journal of Vibration and Acoustics*, 1991, 113(2): 230-234.
[38] G R Liu, X Han, Y G Xu, et al. Material characterization of functionally graded material by means of elastic waves and a progressive-learning neural network. *Composites Science and Technology*, 2001, 61(10): 1401-1411.
[39] G R Liu, K Y Lam, X Han. Determination of elastic constants of anisotropic laminated plates using elastic waves and a progressive neural network. *Journal of Sound and Vibration*, 2002, 252(2): 239-259.
[40] G R Liu, Z C Xi. *Elastic waves in anisotropic laminates*. Boca Raton: CRC Press, 2001.
[41] L W Schmerr. *Fundamentals of ultrasonic nondestructive evaluation*. Switzerland: Springer, 2016.
[42] Z Wei, L K Weavers. Combining COMSOL modeling with acoustic pressure maps to design sono-reactors. *Ultrasonics Sonochemistry*, 2016, 31: 490-498.
[43] L Wang, L Zhao, Z Jiang, et al. High accuracy comsol simulation method of bimorph cantilever for piezoelectric vibration energy harvesting. *AIP Advances*, 2019, 9(9): 095067.
[44] M Friswell, J E Mottershead. *Finite element model updating in structural dynamics.* Berlin Heidelberg: Springer, 1995.
[45] C Mares, J E Mottershead, M I Friswell. Stochastic model updating: Part 1—theory and simulated example. *Mechanical Systems and Signal Processing*, 2006, 20(7): 1674-1695.
[46] J E Mottershead, M Link, M I Friswell. The sensitivity method in finite element model updating: A tutorial. *Mechanical Systems and Signal Processing*, 2011, 25(7): 2275-2296.
[47] Y Sun, S Ding, Z Zhang, et al. An improved grid search algorithm to optimize SVR for prediction. *Soft Computing*, 2021, 25(7): 5633-5644.
[48] M Bilgehan, P Turgut. Artificial neural network approach to predict compressive strength of concrete through ultrasonic pulse velocity. *Research in Nondestructive Evaluation*, 2010, 21(1): 1-17.
[49] G R Liu, S Y Duan, Z M Zhang, et al. Tubenet: A special trumpetnet for explicit solutions to inverse problems. *International Journal of Computational Methods*, 2020, 18(01): 2050030.
[50] S Y Duan, X Han, G R Liu. Two-way trumpetnets and tubenets for identification of material parameters. *Artificial Intelligence for Materials Science*, 2021, 312: 59-91.
[51] J Ma, S Dong, G Chen, et al. A data-driven normal contact force model based on artificial neural network for complex contacting surfaces. *Mechanical Systems and Signal Processing*, 2021, 156: 107612.